International Journal of Mechanical, Industrial and Aerospace Sciences
ISSN: 2517-9950
Vol:7, No:6, 2013

# Numerical Study of Liquefied Petroleum Gas Laminar Flow in Cylindrical Elliptic Pipes

Olumuyiwa A. Lasode, Tajudeen O. Popoola, and B. V. S. S. S. Prasad

***Abstract*—**Fluid flow in cylinders of elliptic cross-section was investigated. Fluid used is Liquefied petroleum gas (LPG). LPG found in Nigeria contains majorly butane with percentages of propane. Commercial available code FLUENT which uses finite volume method was used to solve fluid flow governing equations. There has been little attention paid to fluid flow in cylindrical elliptic pipes. The present work aims to predict the LPG gas flow in cylindrical pipes of elliptic cross-section. Results of flow parameters of velocity and pressure distributions are presented. Results show that the pressure drop in elliptic pipes is higher than circular pipe of the same cross-sectional area. This is an important result as the pressure drop is related to the pump power needed to drive the flow. Results show that the velocity increases towards centre of the pipe as the flow moves downstream, and also increases towards the outlet of the pipe.

***Keywords*—**Elliptic Pipes, Liquefied Petroleum Gas, Numerical Study, Pressure Drop.

## I. Introduction

NIGERIA is a producer of crude oil and petroleum products. It also produces large volume of associated gas rich in natural gas liquids (NGL) and Liquefied petroleum gas (LPG). It has a proven reserve of gas estimated to be about 190 trillion standard cubic feet in 2005 which makes Nigeria one of the largest reserves in the world [1]. Nearly half of this is flared. The quantity of Liquefied petroleum gas (LPG) is estimated to be 4 million tons in 2003 [2]. LPG is extracted from crude oil and natural gas. Natural gas purification produces about 55 percent of all LPG while crude oil refining produces about 45 percent worldwide [3]. LPG gas is widely recognized as a fuel that is clean, versatile, environment friendly and easily transportable. Its main composition is hydrocarbon containing 3 (propane, $C_3H_8$) to 4 (butane, $C_4H_{10}$) carbon atoms depending on the source. It is a gas at atmospheric pressure but can be liquefied when pressure is applied or when the temperature is sufficiently reduced and it is stored in steel containers, cylinders or tanks. When the LPG is being used, some of the pressure in the container is released. Some of the LPG then boils to produce vapor, the heat needed for this being latent heat of vaporization which is taken from the surrounding [4].

The composition of liquefied petroleum gas (LPG) commonly available in Nigeria is a mixture of propane and butane with the percentage varying between 1.4/98.5 to 23.0/76.9 propane/butane depending on the refinery [5].

Study undertaken by World Bank Oil and Gas Division revealed very low per capital usage of LPG gas in Nigeria in comparison to other neighboring countries in West Africa [6]. Consumption collapsed to 50,000 tons in 2003. Most of this was imported. The average consumption rate in Nigeria is estimated to be 0.5kg/h/year while in the other Africa sub-region, it is 3.7kg/h/year. Low level of its usage in Nigeria stems from the fact that the supply is not reliable. It is also not easily accessible and the cost is high.

The main mode of transporting LPG is by either using special pressure containers or by transporting them to storage areas through piping. Knowledge of the flow behavior of the fluid in different geometries will assist in many ways in designing these pipes and also to know the pumping power necessary for pumping the fluid from point of extraction to point of refining and distribution. The circular duct is the most widely used geometry in fluid flow and heat transfer devices [7]. Most pipelines are built with circular cross-section because it has simpler geometry with lower pressure drop during flow [8]. Flow in pipes is a typical example of internal flow. Internal flows are of paramount interest in engineering because of its various applications ranging from the design of heat exchangers to oil and gas pipelines. Elliptic geometry is a useful family of ducts that vary from narrow lenticular passage to a circular one [7]. There is limited knowledge of the fluid flow field in this kind of duct surface. An understanding of the velocity field and the pressure drops in pipe with LPG flowing through it will help in the design of the pipes. References [7] and [9] have presented various results on hydro dynamically developing and developed flow in ducts of various cross sections. Reference [8] also presented their work on natural gas laminar flow in cylindrical pipes with elliptic cross-sections. Their results show velocity and pressure prediction for various aspect ratios. Reference [10] presented a numerical approach solution of control volume to solve fluid flow problem in elliptic duct. They considered aspect ratios with a range of 0.1 to 0.99. Their results shows that the ratio of the entry length in an elliptic duct to that in circular duct with radius equal to semi-major axis of elliptic duct is nearly equal to the aspect ratio of the duct. The total pressure defect was also found to be independent of aspect ratio. Reference [11]

O. A. Lasode is with the Department of Mechanical Engineering, University of Ilorin, P.M.B. 1515, Ilorin 240003, Nigeria. (Corresponding author: +234-805-564-7409; e-mail: oalasode@unilorin.edu.ng)

O. T. Popoola is with Department of Mechanical Engineering, University of Ilorin, P.M.B. 1515, Ilorin 240003, Nigeria. (e-mail: otpopoola@unilorin.edu.ng). This author wishes to acknowledge the Centre for Cooperation in Science and Technology among Developing Societies (CCSTDS-Fellowship no: D.O./CCSTDS/2685/2010), India and Indian Institute of Technology, Madras (IITM) for their financial support and opportunity to do major part of this work in India.

B.V.S.S.S. Prasad is with Department of Mechanical Engineering, Indian Institute of Technology, Madras, India (e-mail: prasad@iitm.ac.in)

used closed form analytic approach to study laminar flow of Newtonian fluid in the entrance region of elliptic ducts. The analysis entails solution of integral forms of mass and momentum balance equations is based on Karma-Pohlhausen integral method. The result shows that pressure defect is independent of aspect ratio. The current paper aims at investigating fluid flow of LPG gas in cylindrical pipes of elliptic cross-sections.

## II. Mathematical Modeling

### *A. Description of Physical Model and Basic Assumptions*

The physical model is shown in Fig. 1. It consists of a straight cylindrical pipe with unchanging cross-section. Its length is Z while semi-minor and semi-major diameters are $L_1$ and $L_2$ respectively. Liquefied Petroleum gas is made to flow through the pipe.

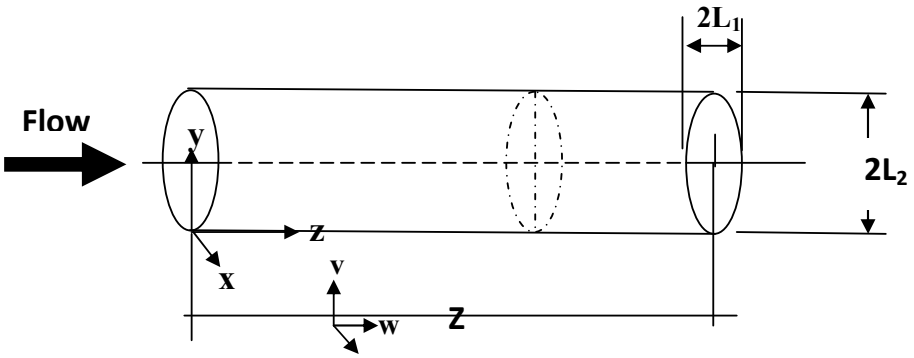


Fig. 1 Physical model and coordinate system of the cylindrical pipe

### *B. Basic Assumptions*

The flow is assumed to be laminar, steady, three dimensional, and incompressible. The fluid is Newtonian with constant thermo-physical properties. The pipe is assumed to be smooth, non-porous, rigid and stationary.

The conservative equations that govern fluid flow in a pipe of cylindrical cross section is given as [12]:

Conservation of Mass

$$\frac{\partial \rho}{\partial t} + \nabla . \rho \vec{v} = 0 \tag{1}$$

where $\vec{v}$ = (u, v, w) is the fluid velocity vectors, $\vec{\rho}$ is the fluid density and t is the time.

The Conservation of momentum equation is

$$\frac{\partial}{\partial t}(\rho \vec{v}) + \nabla . (\rho \vec{v} \vec{v}) = -\nabla P + \nabla . \overline{\overline{\tau}} + \rho g + \vec{F} \tag{2}$$

where P is the static pressure, $\overline{\overline{\tau}}$ is the stress tensor and $\vec{F}$ is the body force.

The stress tensor is given as

$$\overline{\overline{\tau}} = \mu \left[ (\nabla \vec{v} + \nabla \vec{v}^{T}) - \frac{2}{3} \nabla . \vec{v} I \right] \tag{3}$$

where $\vec{v}$ is the velocity, $\mu$ is the molecular viscosity, $I$ is the unit tensor, and the second term on the right hand side is the effect of volume dilation

The following boundary conditions were applied

$$u = v = 0 \text{ and } w = w_0 = 0.0186252 \text{ for } \forall \text{ (x, y)}$$

$$u = v = w = 0 \text{ for } \forall \text{ (x, y) } \frac{x^2}{L_2} + \frac{y^2}{L_1} = 1$$

parabolic outlet condition in z = c

where u,v,w are the velocities along the x,y,z directions respectively.

In the fully developed region, the velocity distribution of a laminar monophase fluid flow in cylindrical elliptic ducts with origin at z is given as [7], [8]

$$w(x,y) = \frac{1}{2\mu}\left(\frac{-\partial P}{\partial Z}\right)\frac{L_1^2 L_2^2}{L_1^2 + L_2^2}\left(1 - \frac{y^2}{L_1^2} - \frac{x^2}{L_2^2}\right) \tag{4}$$

Or

$$\frac{w}{w_m} = 2\left(1 - \frac{x^2}{L_1^2} - \frac{y^2}{L_2^2}\right) \tag{5}$$

where $w_m$ is the average velocity

$$w_m = \frac{1}{4\mu}\left(\frac{-\partial P}{\partial Z}\right)\left(\frac{L_1^2}{1 + \left(\frac{L_1}{L_2}\right)^2}\right) \tag{6}$$

The cross-sectional area, A, perimeter, p, and the hydraulic diameter, $D_h$ are given as [7], [8]

$$A = \pi L_1 L_2 \tag{7}$$

$$\hat{P} = 4L_2 E\left(1-\left(\frac{L_1}{L_2}\right)^2\right) \tag{8}$$

$$D_h = \frac{\pi L_1}{E\left(1-\left(\frac{L_1}{L_2}\right)^2\right)} \tag{9}$$

where is E is the complete elliptic integral of the second kind and details of this can be seen elsewhere [13].

The hydrodynamic entrance length $L_{her}$ and the Fanning friction factor $f_{fdr}$ in the fully developed region are as given by [7], [8]:

$$L_{her} = \frac{0.5132}{\left(1+\left(\frac{L_1}{L_2}\right)^2\right)}\left[\frac{E\left(1-\left(\frac{L_1}{L_2}\right)^2\right)}{\pi}\right]^2 D_h \,\mathrm{Re}_{Dh} \tag{10}$$

$$f_{fdr}\,\mathrm{Re}_{Dh} = 2\left(1+\left(\frac{L_1}{L_2}\right)^2\right)\left[\frac{\pi}{E\left(1-\left(\frac{L_1}{L_2}\right)^2\right)}\right] \tag{11}$$

where Reynolds number

$$\mathrm{Re}_{Dh} = \rho w_m D_h \Big/ \mu \tag{12}$$

At the hydrodynamic entrance region, the apparent friction factor ($f_{her}$) incorporates the combined effects of wall shear and the change in the momentum flow rate due to developing velocity profile based on the total axial pressure drop from the duct inlet (at z = 0) to the local point of interest. This is given as [7], [8]:

$$\Delta P^*_{her} = \frac{P_{z=0} - P}{\rho w_m^2 \Big/ 2} = f_{her}\frac{4z}{D_h} \tag{13}$$

The incremental pressure drop number in the hydrodynamical developing region K(z) is

$$K(z) = (F_{her} - F_{fdr})\frac{4z}{D_h} \tag{14}$$

K(z) is sometimes referred to as the incremental pressure defect. It increases monotonically from a value of zero at z=0 to a constant value K(∞) at z>$L_{her}$ [7], [8]

The equation that relates the incremental pressure drop number, friction factor, the axial pressure drop is given here following [8]:

$$\Delta P^*_{her} = f_{her}\mathrm{Re}_{Dh}\left(\frac{4z}{D_h \mathrm{Re}_{Dh}}\right) = K(z) + f_{fdr}\mathrm{Re}_{Dh}\left(\frac{4z}{D_h \mathrm{Re}_{Dh}}\right) \tag{15}$$

The apparent friction factors and incremental pressure drop numbers can be expressed as:

$$f_{her}\,\mathrm{Re}_{Dh} = \frac{\Delta P^*_{her}}{4\left(\frac{4z}{D_h\,\mathrm{Re}_{Dh}}\right)} \tag{16}$$

where

$$\Delta P^*_{her} = \frac{2(1-\eta)(1+3\eta) - (1+\eta)^2 \ln \eta^3}{3(1+\eta)^2} \tag{17}$$

and

$$K(z)_{her} = \frac{(3\eta^3 + 9\eta^2 + 21\eta + 7)(1-\eta)}{6(1+\eta)^2} \tag{18}$$

η is a boundary layer parameter that refers to the friction of the duct cross-section carrying inviscid flow [7].

The term η is implicitly obtained from (19) as a function of z:

$$16\left(1+\left(\frac{L_1}{L_2}\right)^2\right)\left[\frac{\pi}{E\left(1-\left(\frac{L_1}{L_2}\right)^2\right)}\right]^2 \frac{z}{D_h\,\mathrm{Re}_{Dh}} = \eta^2 - 1 - \ln\eta^2 \tag{19}$$

The fully developed incremental pressure drop number K(∞) for elliptic ducts has been found to be independent of the duct aspect ratio ($L_1/L_2$). The value of K(∞) is recommended to be 1.26 for practical calculations [8].

η attains the value of zero as the limit of the flow becomes hydrodynamically developed and all the momentum transfer quantities asymptotically reduce to the known exact fully developed values [7].

## III. Numerical Procedure

Commercial available CFD software code FLUENT (version 6.3.26) was used to simulate the 3D motion of fluid through horizontal elliptic duct. The grids were generated using ANSYS ICEM CFD (version 12.0.1) which is the pre-processing module of the FLUENT code. The geometry and the grid for the pipes are then imported into FLUENT. FLUENT uses finite volume method. It can use both structured and unstructured meshes. The geometries considered are cylindrical pipes of elliptic cross sections with lengths 30m. For the solution control, under the pressure-velocity coupling, SIMPLE was used. Under discretisation, for pressure, standard was used and for momentum, first order upwind was used. A convergence criterion of $10^{-10}$ was used for continuity and x, y and z components of Navier Stokes equation.

## IV. Results and Discussion

### A. Numerical Grid

Figs. 2 to 6 give the details of the grids used for the cylindrical pipe of elliptic cross section. The mesh is hexahedral. The final grids were obtained after several refinements called grid independent study. Table I gives the dimensions of the pipes used in the current work.

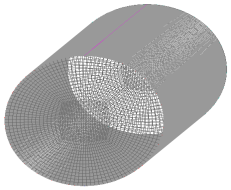

Fig. 2 Details of circular grid with 456000 elements (Pipe 1)

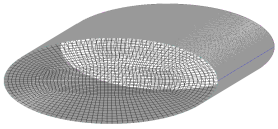

Fig. 3 Details of elliptic grid with 467161 elements (Pipe 2)

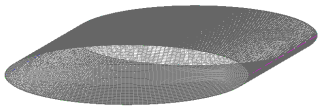

Fig. 4 Details of elliptic grid with 343035 elements (Pipe 3)

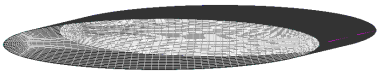

Fig. 5 Details of elliptic grid with 485817 elements (Pipe 4).

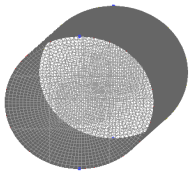

Fig. 6 Details of circular grid with 470000 elements (Pipe 5)

TABLE I
Dimensions of the Pipes Used in the Current Work

| Pipe | Pipe Dimensions (m) | | |
|---|---|---|---|
| | $L_1$ | $L_2$ | C |
| 1 | 0.100 | 0.100 | 30.00 |
| 2 | 0.100 | 0.150 | 30.00 |
| 3 | 0.100 | 0.300 | 30.00 |
| 4 | 0.100 | 0.500 | 30.00 |
| 5 | 0.173205 | 0.173205 | 30.00 |

### B. Numerical Validation

Table II depicts the properties of the gas phase used for the validation of the current work. Pipe 1($L_1$=$L_2$=0.1m) was used for the simulation with velocity $w_o$ = 0.1m/s. Results from the numerical results taken at distance 25m from the inlet was compared with analytic result from [7] and numerical result of [8]. Fig. 7 shows the comparison. The result shows good agreement with error of 0.24% when compared with result of [7] at y=0 which is the axis with maximum velocity. Table III compares the natural gas flow pressure drop between [7], [8] and the current work for the purpose of validation. The range of error obtained from [8] is found to vary between 4.77 to 20.33%, while the current work varies between 0.58 to 13.5%.

TABLE II
Physical Properties of the Natural Gas Used in Validation [8]

| $\rho$ (kg/m$^3$) | $\mu$ (N.s/m$^2$) at 1 atm and 20$^o$C |
|---|---|
| 0.72 | $1.1 \times 10^{-5}$ |

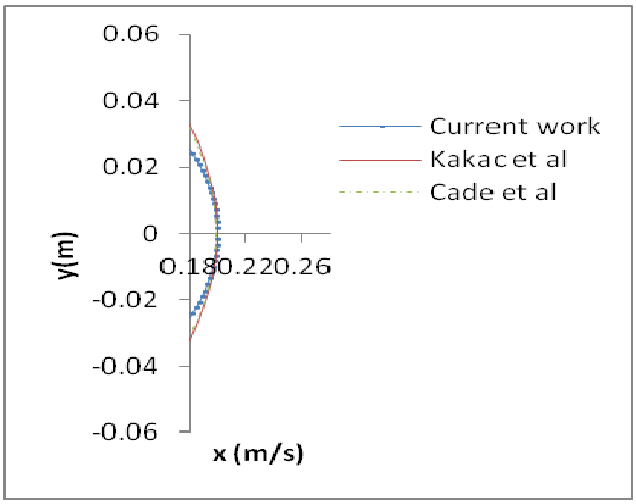


Fig. 7 Graph of velocity distribution at 25m along pipe1

TABLE III
Natural Gas Flow Pressure Drop Obtained for Validation of the Current Work

| $L_1xL_2xC$ (mxmxm) | Kakac *et al* [7] (N/m$^2$) | Cade *et al* [8] (N/m$^2$) | Current work (N/m$^2$) |
|---|---|---|---|
| Pipe1=0.1x0.1x30 | 0.030599 | 0.032060 | 0.0307772 |
| Pipe2=0.1x0.15x30 | 0.023265 | 0.025226 | 0.0237164 |
| Pipe3=0.1x0.3x30 | 0.018865 | 0.021516 | 0.0192670 |
| Pipe4=0.1x0.5x30 | 0.017926 | 0.021571 | 0.0203506 |
| Pipe5=0.173205x0.173205x30 | 0.012709 | 0.014347 | 0.0132434 |

### C. Applications

The physical property of LPG gas used for the current work is depicted in Table IV. It is worthy of note that the formulas used in arriving at the dynamic viscosities and densities in Table IV can be found in [13].

The result of the simulations of 100 percent butane are shown in Fig. 8 all through to Fig. 29 while Table V depicts the pressure drop results of varying percentages of butane/propane which are the major constituents of LPG. Figs. 8 to 11 (pipe1), Figs. 14 to 17 (pipe2), Figs. 18 to 21 (pipe3), Figs. 22 to 25 (pipe4) and Figs. 26 to 29 (pipe 5) show the velocity field of the 100 percent LPG gas phase at cross sections yx at z= 0.5m, 5m, 10m and 30m respectively. In all cases, it is observed that the velocity at the wall is zero

confirming the no slip condition. The velocity is seen to increase from walls towards the centre of the pipe and also increases downstream as the fluid flows from close to the inlet (at 0.5m) towards the outlet (at 5m, 10m and 30m). The outlet velocity appeared to be at maximum. Edge effects are detected in pipes with large aspect ratios just as reported by [7]. This is caused by curvature of the pipes**.**

Figs. 12 and 13 show typical velocity and pressure variations in the axial plane yz along pipe1. It is observed that velocity increases towards the centre and along the plane while the pressure on the other hand decreases towards the downstream along the plane**.**

For comparison of pressure drop between two ducts, pipe 3 ($L_1$=0.1 m and $L_2$=0.3 m) and pipe 5 ($L_1$=$L_2$=0.173205) are compared. The two pipes are of the same cross sectional area. Pipe 3 is elliptic while pipe 5 is circular. Table V shows the results of pressure drop of various aspect ratios at different percentage of Butane. The result shows that the pressure drop in the elliptic pipe is 0.0022836 Pa while that of the circular pipe is 0.001569387 Pa. The pressure drop by pipe 3 is therefore higher than that of pipe5 by 45.5%. This implies that in order to maintain the flow of LPG in pipe 3 the pressure drop has to be higher than that of the pipe 5 by the said percentage for the same flow rate.

TABLE IV
PHYSICAL PROPERTIES OF THE LPG USED FOR THE SIMULATION

| Butane (%) | Propane (%) | $\mu$ (N.s/m$^2$) | $\rho$ (x10$^{-6}$) (kg/m$^3$) |
|---|---|---|---|
| 100 | 0 | 2.460 | 7.000 |
| 95 | 5 | 2.433 | 7.533 |
| 90 | 10 | 2.405 | 8.010 |
| 85 | 15 | 2.378 | 8.435 |
| 80 | 20 | 2.350 | 8.811 |

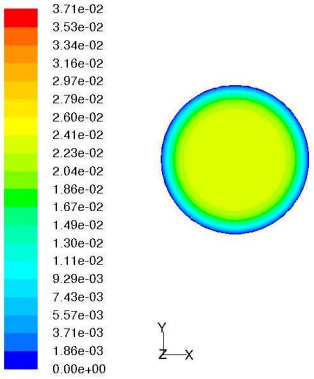


Fig. 8 Velocity distribution of 100% butane in the cross-section yx in z =0.5m along the Pipe 1

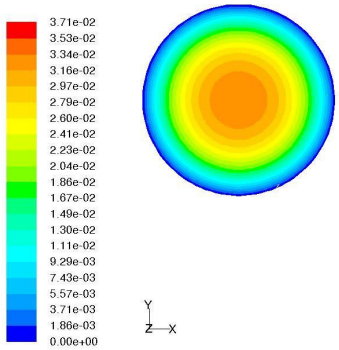


Fig. 9 Velocity distribution of 100% butane in the cross-section yx in z =5m along the Pipe 1

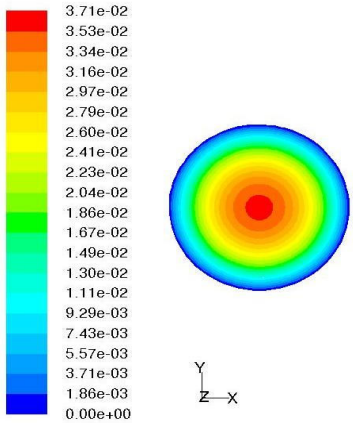


Fig. 10 Velocity distribution of 100% butane in the cross-section yx in z =10m along the Pipe 1

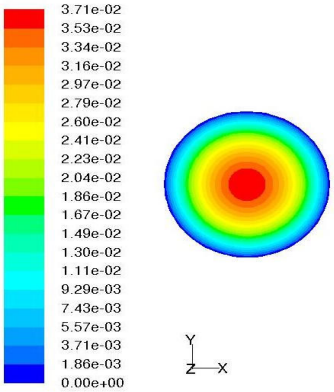


Fig. 11 Velocity distribution of 100% butane in the cross-section yx in z =30m along the Pipe 1

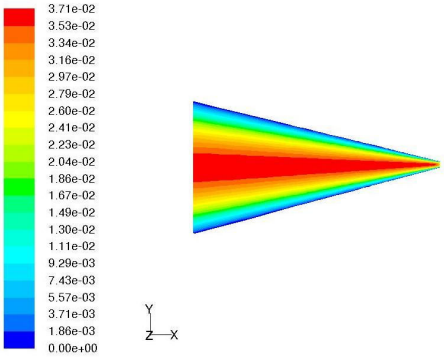


Fig. 12 Typical Velocity distribution for 100% butane in the axial plane yz along Pipe 1

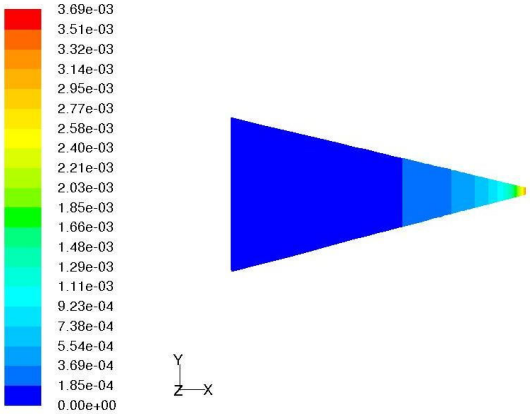


Fig. 13 Typical Pressure distribution for 100% butane in the axial plane yz along Pipe 1

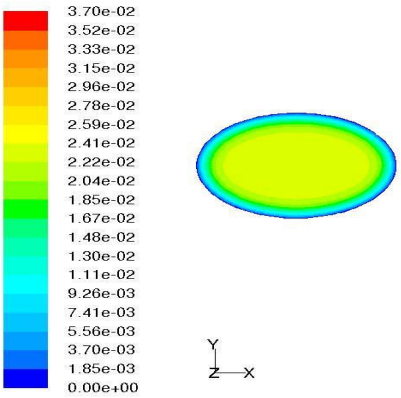


Fig. 14 Velocity distribution of 100% butane in the cross-section yx in z =0.5m along the Pipe 2

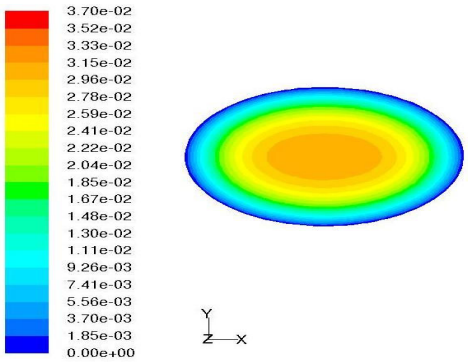


Fig. 15 Velocity distribution of 100% butane in the cross-section yx in z =5m along the Pipe 2

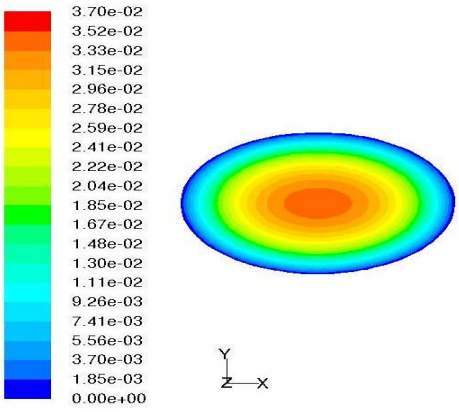


Fig. 16 Velocity distribution of 100% butane in the cross-section yx in z =10m along the Pipe

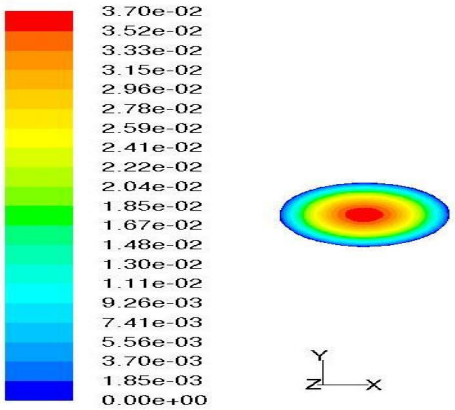


Fig. 17 Velocity distribution of 100% butane in the cross-section yx in z =30m along the Pipe 2

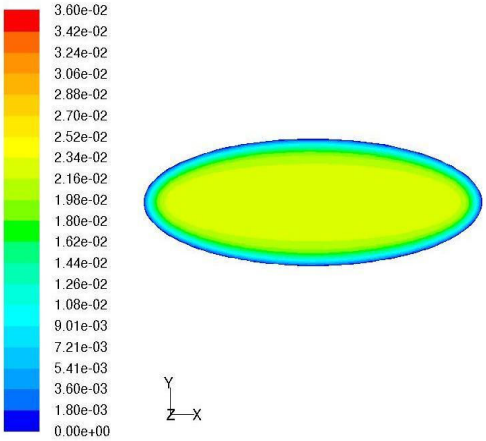


Fig. 18 Velocity distribution of 100% butane in the cross-section yx in z =0.5m along the Pipe 3

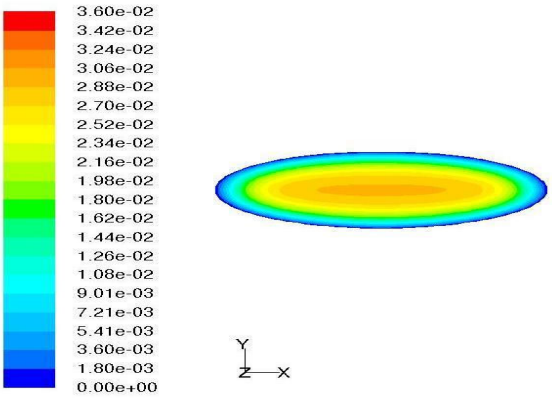


Fig. 19 Velocity distribution of 100% butane in the cross-section yx in z = 5m along the Pipe 3

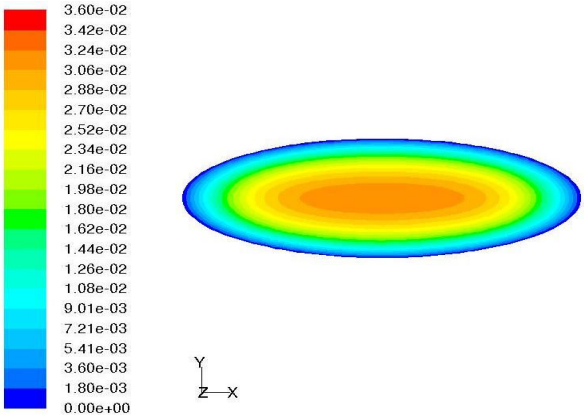


Fig. 20 Velocity distribution of 100% butane in the cross-section yx in z =10m along the Pipe 3

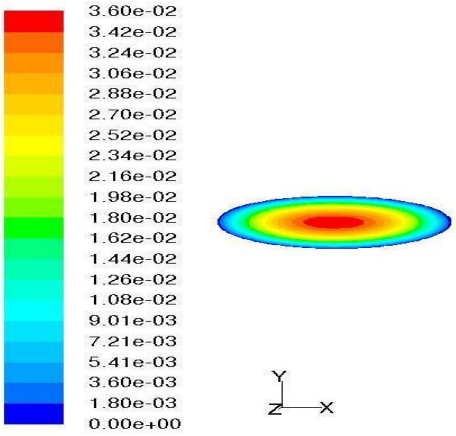


Fig. 21 Velocity distribution of 100% butane in the cross-section yx in z =30m along the Pipe 3

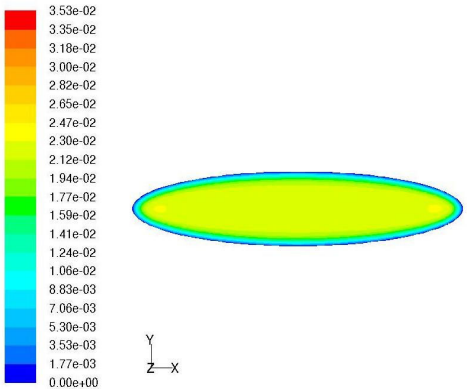


Fig. 22 Velocity distribution of 100% butane in the cross-section yx in z =0.5m along Pipe 4

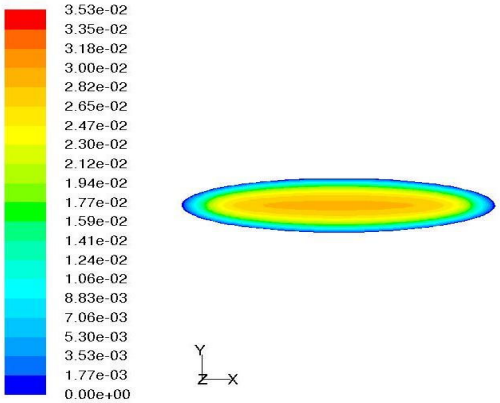


Fig. 23 Velocity distribution of 100% butane in the cross-section yx in z =5m along the Pipe 4

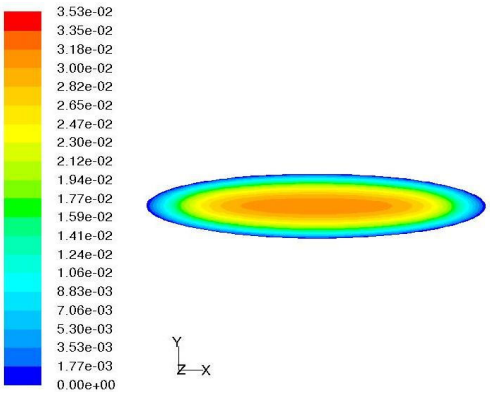


Fig. 24 Velocity distribution of 100% butane in the cross-section yx in z =10m along the Pipe 4

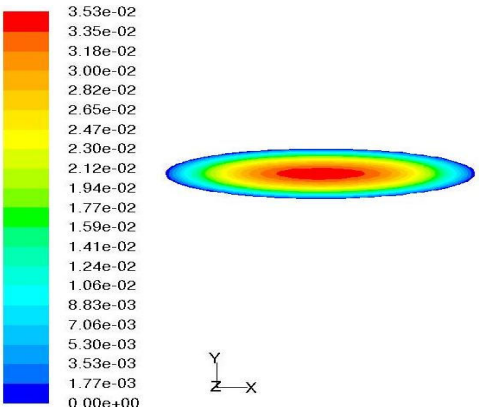


Fig. 25 Velocity distribution of 100% butane in the cross-section yx in z =30m along the Pipe 4

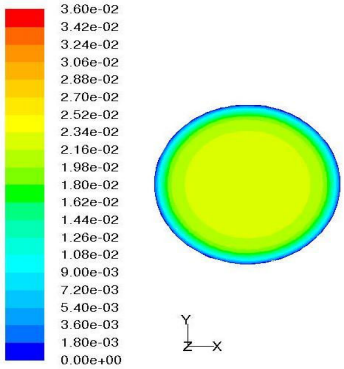


Fig. 26 Velocity distribution of 100% butane in the cross-section yx in z =0.5m along the Pipe 5

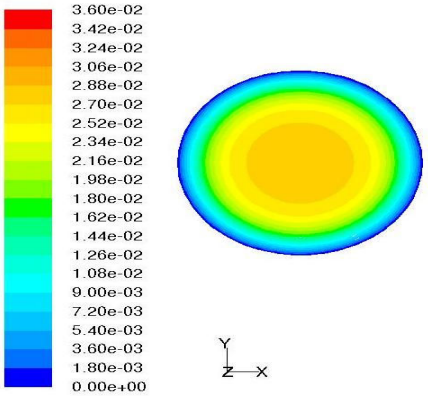


Fig. 27 Velocity distribution of 100% butane in the cross-section yx in z =5m along the Pipe 5

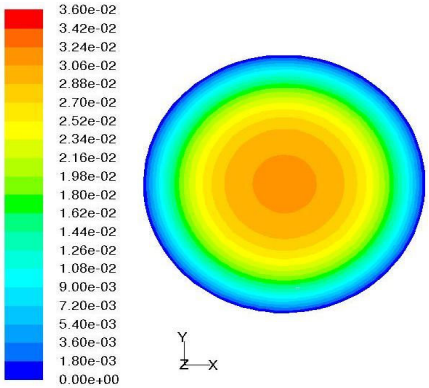


Fig. 28 Velocity distribution of 100% butane in the cross-section yx in z =10m along the Pipe 5

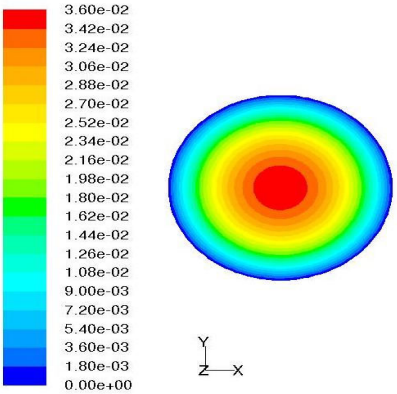


Fig. 29 Velocity distribution of 100% butane in the cross-section yx in z =30m along the Pipe 5

The pressure drop variation of LPG (Butane/Propane) was observed to be an order of magnitude less than that observed for natural gas. The implication of this is that lower pressure drop is needed to maintain LPG flow in the pipes than natural gas flow in the pipe of the same dimension. Another observation from Table V is that as $L_2$ value is increased with $L_1$ remaining constant, the pressure drop reduces for all

percentages of Butane/propane mix. In all pipes, the least pressure drop is experienced in LPG with 100/0 % (butane/propane) contents.

TABLE V
PRESSURE DROP VARIATIONS OF ASPECT RATIOS AND PERCENTAGE BUTANE TO PROPANE

| Butane/Propane (%) | Pipe1 | Pipe2 | Pipe3 | Pipe4 | Pipe5 |
|---|---|---|---|---|---|
| 100/0 | 0.00368498 | 0.00281098 | 0.00228360 | 0.00214675 | 0.00156939 |
| 95/5 | 0.00431589 | 0.00329227 | 0.00267459 | 0.00251432 | 0.00183810 |
| 90/10 | 0.00493578 | 0.00376513 | 0.00305874 | 0.00287544 | 0.00210209 |
| 85/15 | 0.00553677 | 0.00422570 | 0.00345052 | 0.00322556 | 0.00235806 |
| 80/20 | 0.00611201 | 0.00466240 | 0.00378767 | 0.00355927 | 0.00260305 |

## V. CONCLUSION

The software FLUENT has been used to predict the 3 dimensional fluid flow in cylindrical pipes of elliptic cross-section. Results show that pressure drop in elliptic pipes is higher than in circular pipes. It also shows that pressure drop in pipes with natural gas flow is an order of magnitude greater than pressure drop in LPG gas flow. It can also be concluded that as the ratio of aspect ratios ($L_1/L_2$) decreases the pressure drop reduces. The velocity of the LPG flow decreases as the aspect ratio become smaller.

## VI. RECOMMENDATION

It is recommended based on the results that LPG with 1.6/98.5 % propane/ butane composition be encouraged in Nigeria to reduce pumping power requirement. Further work is on going to compute the heat transfer characteristics of the LPG flow in pipelines.

## REFERENCES

[1] C.C. Chikwendu, "Change-over from Kerosene to LPG use – A family case study", Energia: International Network on Gender and Sustainable Energy, January 2011.
[2] B. Agboade, "The International Comparative Legal Guide to Gas Regulation 2012" London: Global Legal Group Ltd, 2012, p. 215.
[3] http://www.window.state.tx.us/specialrpt/energy/pdf/06-LPG.pdf, Energy Report, Texas Comptroller of Public Account, 2008, Accessed online on 12/12/2012.
[4] http://www.ripack.in/pdf/LPG.PDF, Accessed online on 12/12/2012.
[5] J.A. Olorunmaiye, "Tuning of Valveless PulsedCombustor Running on Nigerian Liquefied Petroleum Gas", *Centrepoint: A Journal of Intellectual Scientific and Cultural Interest, Science Edition,* vol. 7, no. 1, 1997, pp. 1-15.
[6] World Bank Oil and Gas division and World LPG Gas Association, 2001.
[7] [R.K. Shah, M.S. Bhatti, "Laminar convective heat transfer in ducts," in *Handbook of Single-Phase Convective Heat Transfer*, S. Kakaç, W. Aung, R.K. Shah, Eds. New York: John Wiley and Sons, 1987, pp.3.1-3.137.
[8] M.A. Cade, W.C. Lima, P.B. Farias-Neto, A.G.B. Lima, "Natural Gas Laminar Flow in Elliptic Cylindrical Pipes: A Numerical Study", *Brazilian Journal of Petroleum and Gas*, vol. 4, no.1, 2010, pp. 19-33.
[9] W.M. Rohsenow, J.P. Harnett, *Handbook of Heat Transfer*. New York: McGraw-Hill Book Company, 1973.
[10] K. Velusamy, V. K., Garg, "Entrance flow in elliptic ducts" *International Journal for Numerical Methods in Fluids*, vol. 17, 1993, pp. 1079–1096.
[11] M.S. Bhatti, "Laminar flow in the entrance region of elliptical ducts" in *Proc. ASME Applied Mechanics, Bioengineering, and Fluids Engineering Conference*, Houston, June 1983.
[12] FLUENT 6.3 Users Manual (2006)
[13] L.M. Milne-Thomson, "Elliptic Integrals", In Handbook of Mathematical Functions, 9th ed. M. Abramowitz, I.A. Stegun, Eds. New York: Publications, Inc., 1972, p. 1046.